ORIGINAL ARTICLE

Veterinary Research Forum. 2025; 16 (12): 691 - 698
doi: 10.30466/vrf.2025.2060636.4759
Journal Homepage: vrf.iranjournals.ir

Veterinary Research Forum

Morphometrical study of Luristan newt (*Neurergus kaiseri*) vertebral column with micro-CT scan

Yasin Valizadeh[1], Mohammad Nasrolahzadeh Masouleh[1]*, Omid Zehtabvar[2], Saied Bokaie[3]

[1] Department of Veterinary Clinical Sciences, SR.C., Islamic Azad University, Tehran, Iran; [2] Department of Basic Sciences, Faculty of Veterinary Medicine, University of Tehran, Tehran, Iran; [3] Department of Food Hygiene, Faculty of Veterinary medicine, University of Tehran, Tehran, Iran.

Article Info

Article history:

Received: 31 May 2025
Accepted: 12 October 2025
Available online: 15 December 2025

Keywords:

Anatomy
Kaiser's mountain newt
Micro-CT scan

Abstract

Vertebrate skeletons can be considered as a combination of apparently separate units, which has attracted the attention of comparative anatomists. The Luristan newt (*Neurergus kaiseri*) is one of the newt species native to Iran, inhabiting a limited area in the southern Zagros Mountain range. The present study investigated the typical morphometrical characteristics of the normal, mature, and healthy Luristan newt vertebral column using micro-computed tomography (micro-CT). For this study, five female and five male specimens of Luristan newt were utilized. The typical morphological characteristics of the vertebral column were then examined. To facilitate the description of different regions of the vertebral column, abbreviations were employed: "T" for trunk vertebrae, "S" for sacral vertebrae, "Cd-S" for caudosacral vertebrae, and "Cd" for caudal vertebrae. All parameters, including vertebral body height, vertebral body length, spinous process height, spinal canal width, and spinal canal height, exhibited significant differences throughout the vertebral column. The highest vertebral body height in both sexes was recorded in T_{10}. The highest vertebral body length in both sexes was observed in T_{12}. The highest spinous process height in both sexes was recorded in Cd_3. The highest spinal canal width in both sexes was recorded in the atlas**.** The maximum spinal canal height in both sexes was also recorded in the atlas. The lowest values in all parameters were observed in the last caudal vertebra. This study presents a comprehensive description and morphometric evaluation of the vertebral column in Luristan newt with micro-CT.

Introduction

The vertebral column consists of a series of distinct repeating cartilaginous or bony elements. The skeletal system of vertebrates and its elements are crucial in evolutionary biology.[1] Moreover, skeletal structures contain biological information that can be used to determine species type, age, sex, size, and even the environmental conditions of their habitat.[2]

The vertebral column first appeared with evidence of segmented blocks along a notochord in the fossils of *Haikouella* and *Haikouichthys*. In lampreys, several small cartilaginous elements, including neural arches and spines, are positioned atop a prominent notochord; however, the main vertebral bodies are absent. The first vertebral components to emerge were the dorsal and ventral arches, being positioned over the notochord. The neural tube was safeguarded by the dorsal arches, which included both the neural and inter-neural arches. Conversely, the ventral arches, namely the hemal and inter-hemal arches, surrounded the blood vessels. The next step in the development of the fundamental components of a vertebra was the creation of two centra, including the inter-centrum (or hypo-centrum) and pleuro-centrum. These centra formed where the bases of the ventral arches expanded and made contact with the notochord. The primary function of the centra was to anchor and support the arches.[3]

In some vertebrates, the centrum may be absent, or one or two centra may be present. Each centrum essentially forms the vertebral body. Centra with flat ends are called acoelous and appear to be well-suited for receiving and distributing compressive forces along the vertebral column. If both surfaces are concave, the centrum is classified as amphicoelous, a design allowing for limited movement in multiple directions. Centra that

***Correspondence:**

Mohammad Nasrolahzadeh Masouleh. DVM, DVSc
Department of Veterinary Clinical Sciences, SR.C., Islamic Azad University, Tehran, Iran
E-mail: mnmasouleh@iau.ac.ir

are concave anteriorly and convex posteriorly are termed procoelous, while the reverse shape, concave posteriorly and convex anteriorly, characterizes opisthocoelous centra. In both procoelous and opisthocoelous centra, the convex articular surface of one centrum fits into the concave surface of the adjacent centrum, forming a ball-and-socket joint. This structure enables a wide range of motion in most directions without stretching the nerve cord.[3]

In the freshwater basins of Iran, three genera of newts, including, *Triturus*, *Salamandra*, and *Neurergus*, are found, all belonging to the Salamandridae family.[4] The Luristan newt (*Neurergus kaiseri*) is one of the endemic newt species of Iran, inhabiting the Zagros Mountains. The breeding habitats of *N. kaiseri* include high-altitude streams and ponds, which are often seasonal. With the onset of spring and subsequently summer, these newts migrate to the surrounding rugged mountains.[5]

The *N. kaiseri* primarily inhabits seasonal pools, where water levels fluctuate significantly. This species is distinctly different from other members of the *Neurergus* genus in terms of appearance and morphometry, being notably smaller. Its most distinguishing feature is a broad, somewhat wavy orange dorsal stripe, formed by the fusion of round spots, serving as a key identifying characteristic of this species.[6]

Computed tomography (CT) scan is a three-dimensional (3D) X-ray imaging technique involving projecting X-ray beams at multiple angles around an axis, followed by the application of a tomographic reconstruction algorithm to generate closely spaced cross-sectional images. The volume of 3D images produced by micro-CT scanning ranges from 500 to 2,000 voxels, with each voxel containing at least 8.00-16.00 bits of grayscale information. Consequently, the data load for each 3D image is substantial, making image storage, transmission, visualization, and analysis the critical aspects of the process. The technologies used in micro-CT and standard CT scanners are fundamentally similar; however, they differ in terms of image quality, resolution, and the size of the 3D volume they can capture within a given time frame.[7]

This study aimed to examine the morphometric characteristics of the vertebral column in both male and female Luristan newts, an endangered species. The authors hypothesized that there are significant differences between different parameters in the vertebral column in both sexes.

Materials and Methods

Animals. Due to the special protection status of this species, which is classified as endangered, coordination and communication were established with the relevant organizations to obtain consent for sample collection. Five adults male and five adults female Luristan newts were captured from the region during two separate time periods. The sex of the samples was determined based on cloacal morphology; males exhibited a fleshy protuberance at the cranial end of the valve slit, whereas females lacked this protuberance.[8] To store and transport the samples to the Preclinical Laboratory at Tehran University of Medical Sciences, Tehran, Iran, plastic containers were used. Given that the newt inhabits reservoirs and ponds, the containers were filled with cold water (approximately 17.00 to 20.00 ˚C) and stones were placed outside the water to create a dry and humid environment. As a result, the samples had access to both dry and aquatic environments (Fig. 1). This study was approved by the university's ethics committee under the code IR.IAU.SRB.REC.1403.399; December 14, 2024.

Micro-CT scan. One day after collection, the samples were transferred to the micro-CT scan Department at the Preclinical Laboratory of Tehran University of Medical Sciences, Tehran, Iran. Efforts were made to position the animals for the micro-CT scan (LOTUS-inVivo Micro-CT Scanner, Behin Nagareh Co., Tehran, Iran) in a way that stretched their bodies and ensured the organs were symmetric and also stretched. Care was taken to avoid any organs lying on body, and animals' bodies were positioned parallel to the table. For temporary immobilization, an anesthetic pool of tricaine methane sulfonate (10.00 mg L^{-1} of water, Merck, Darmstadt, Germany) was used.[9] Afterward, adhesive tape was applied to prevent any movement during the micro-CT scanning process. To minimize damage caused by the tape, a tampon layer was first placed on the body of the animal before securing it with the tape (Fig. 1). All samples were placed in a ventral recumbency on the micro-CT scanner table, with their heads directed toward the gantry. Imaging was conducted by the micro-CT scanner. This micro-CT scanner operates within a voltage range of 45.00 to 90.00 kilovolts, offering a field of view and scan length up to the 80.00 × 200 mm and achieving pixel sizes down to the 10.00 µm. It is capable of measuring dimensions at the µm level (Fig. 1).[10]

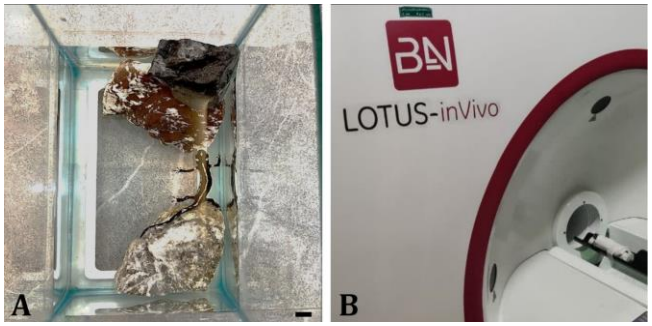

Fig. 1. A) Methods of transporting and storing samples (bar = 10.00 mm), and **B)** The micro-computed tomography scanner and positioning the newt prior the micro-computed tomography scanning.

The technical parameters for radiation and CT scan process were as follows: frame exposure time: 0.25 sec, slice thickness: 0.10 mm, scan angle: 360°, tube Voltage: 80.00 kVp, and tube current: 95.00 µA. One day after the micro-CT scan, the samples were returned to their original habitat. The digital files, saved in Digital Imaging and Communications in Medicine format, were examined and morphologically evaluated using Radiant DICOM Viewer Software (version 2025.1; Medixant, Poznań, Poland). All measurement results were trans-ferred to the SPSS Software (version 31.0; IBM Corp., Armonk, USA) where the mean and standard deviation values for all parameters were calculated and recorded. For each measured parameter, the mean was adjusted by adding and subtracting two standard deviations, thereby determining the reference range, which was the primary objective of this study. The independent samples t-test was used for all formulated hypotheses. The studied parameters are organized in Table 1.

Worthington and Wake, have identified the following five regions in the terrestrial newt: Atlas (cervical vertebra), trunk vertebrae, sacrum, caudo-sacral vertebrae, and caudal vertebrae.[11]

In this study, the vertebral column of the Luristan newt was examined based on this classification. To facilitate the description of different regions of the vertebral column, abbreviations were employed: "T" for trunk vertebrae, "S" for sacral vertebrae, "Cd-S" for caudosacral vertebrae, and "Cd" for caudal vertebrae.

Results

In this section, the vertebral column of the Luristan newt was studied. Also, to illustrate the precise positioning of the vertebrae relative to one another and to provide more detailed insights, 3D reconstructions were performed (Fig. 2). Various parameters mentioned in Table 1 were measured and statistically analyzed, with details presented in Table 2.

Vertebral body height (VBH) analysis. In female specimens, significant differences in VBH were observed only for T_1 compared to the atlas and T_{10} compared to the T_9, where VBH increased in both cases, and Cd_{22} compared to the Cd_{21}, where VBH decreased. For all other vertebrae, the differences in VBH between each vertebra and its adjacent ones were not statistically significant.

Table 1. Anatomical parameters of the vertebral column of *Neurergus kaiseri*.

Parameters	Anatomical descriptions	Visual description
Vertebral body height	Distance from the base of the vertebrae to the vertebral canal in the transverse view; the maximum distance was measured.	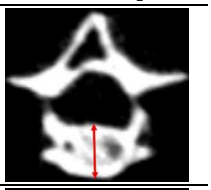
Vertebral body length	The length of the vertebral body in the mid-sagittal view; the maximum distance was measured.	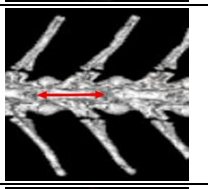
Spinous process height	Distance from the base to the apex of the spinal process; the maximum distance was measured.	
Spinal canal width	Distance between left extremity of vertebral canal and right extremity of vertebral canal in transverse view	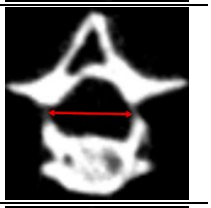
Spinal canal height	Distance between the base of vertebral canal and ventral aspect of dorsal lamina in transverse view	

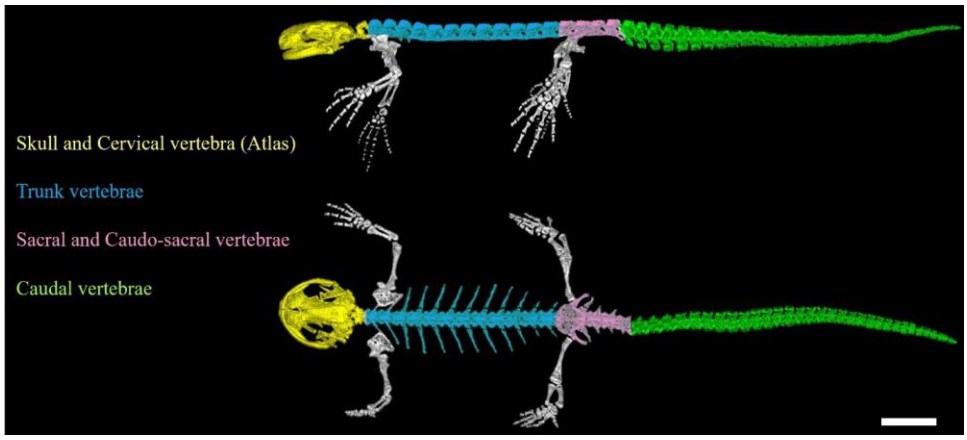

Fig. 2. The volume rendering of micro-computed tomography images of the *Neurergus kaiseri* skeleton, indicating each segment of the vertebral column using Worthington and Wake classification (bar = 10.00 mm).[11]

In male specimens, significant differences in VBH were found for T_1 compared to the atlas and T_{10} compared to the T_9, where VBH increased in both cases. Beyond these points, no statistically significant differences in VBH were observed between adjacent vertebrae throughout the rest of the vertebral column. The highest VBH in both male and female specimens was recorded in T_{10}, while the lowest VBH was observed in the last caudal vertebra.

When comparing VBH between sexes, significant differences were found in T_3, Cd_{12}, Cd_{13}, Cd_{14}, Cd_{15}, Cd_{16}, Cd_{17}, Cd_{18}, Cd_{19}, Cd_{20}, and Cd_{21}, whereas no significant differences were observed in the remaining vertebrae. Specifically, VBH in T_3, Cd_{12}, Cd_{13}, Cd_{14}, Cd_{15}, Cd_{16}, Cd_{17}, Cd_{18}, Cd_{19}, Cd_{20}, and Cd_{21} was greater in females than males, while in all other vertebrae, VBH values were similar between sexes (Table 2).

Vertebral body length (VBL) analysis. In female specimens, significant differences in VBL were observed in the following comparisons: T_1 compared to the atlas, T_2 compared to the T_1, T_3 compared to the T_2, and T_8 compared to the T_7, with VBL increasing progressively. Significant differences in VBL were also observed in the following comparisons: Cd-S_2 compared to the Cd-S_1, Cd_2 compared to the Cd_1, Cd_3 compared to the Cd_2, Cd_{14} compared to the Cd_{13}, and Cd_{18} compared to the Cd_{17}, as well as Cd_{22} compared to the Cd_{21}, Cd_{23} compared to the Cd_{22}, Cd_{24} compared to the Cd_{23}, and Cd_{25} compared to the Cd_{24}, where VBL decreased in all cases. No significant differences were observed betweenT_4 and T_6, T_9 and S_1, Cd_4 and Cd_{12}, and Cd_{15} and Cd_{17}. After Cd_{25}, no further significant differences were observed.

In male specimens, significant differences in VBL were observed in the following comparisons: T_1 compared to the atlas, T_2 compared to the T_1, and T_3 compared to the T_2, with a progressive increase. Significant differences in VBL were also observed in S_1 compared to the T_{12}, Cd-S_2 compared to the Cd-S_1, and Cd_{26} compared to the Cd_{25}, where VBL decreased in all cases. No significant differences were found between T_4 and T_{11}, Cd-S_1 compared to the S_1, and Cd-S_3 compared to the Cd_{24}. After Cd_{26}, no further significant differences were observed. The highest VBL in both sexes was observed in T_{12}, while the lowest VBL was recorded in the last caudal vertebra.

When comparing VBH between sexes, no significant differences between males and females were found in Cd_{18}, Cd_{19}, Cd_{20}, Cd_{21}, Cd_{22}, Cd_{24}, Cd_{26}, Cd_{27}, Cd_{28}, Cd_{29}, Cd_{30}, and Cd_{31}. In contrast, significant differences were observed in other vertebrae. The Cd_{23} and Cd_{25} had higher VBL in males, while all other vertebrae exhibited greater VBL in females (Table 2).

Spinous process height (SPH) analysis. In female specimens, no significant differences were observed in SPH from T_1 to T_9. Significant differences were observed in the following comparisons: T_{11} compared to the T_{10}, where SPH increased, T_{12} compared to the T_{11}, where SPH decreased, and Cd-S_3 compared to the Cd-S_2, Cd_2 compared to the Cd_1, and Cd_3 compared to the Cd_2, where SPH increased in all cases. Additionally, SPH decreased in the following comparisons: Cd_{11} compared to the Cd_{10}, Cd_{19} compared to the Cd_{18}, and Cd_{22} compared to the Cd_{21}. No significant differences were observed in S_1 compared to the T_{12}, Cd-S_1 compared to the S_1, Cd-S_2 compared to the Cd-S_1, from Cd_3 to Cd_9, from Cd_{11} to Cd_{18}, and from Cd_{19} to Cd_{21}. After Cd_{22}, no further significant differences were observed.

In male specimens, no significant differences were observed in SPH from T_1 to T_9. Significant differences were observed in the following comparisons: T_{11} compared to the T_{10}, where SPH increased, T_{12} compared to the T_{11} and S_1 compared to the T_{12}, where SPH decreased in both cases, Cd-S_3 compared to the Cd-S_2, Cd_2 compared to the Cd_1, and Cd_3 compared to the Cd_2, where SPH increased in all cases. Also, SPH decreased in Cd_{22} compared to the Cd_{21} and Cd_{28} compared to the Cd_{27}. No significant differences were observed in Cd-S_1 compared to the S_1, Cd-S_2 compared to the Cd-S_1, Cd_1 compared to the Cd-S_3, from Cd_3 to Cd_{20}, and from Cd_{22} to Cd_{26}. After Cd_{28}, no further significant differences were observed.

Table 2. Micro-computed tomography scanning measurements of morphometric parameters (mm) of *Neurergus kaiseri.* Data are presented as mean ± standard deviation.

Vertebra	VBH		VBL		SPH		SCW		SCH	
	Female	Male	Female	Male	Female	Male	Female	Male	Female	Male
Atlas	0.54 ± 0.02	0.55 ± 0.04	1.65 ± 0.01*	1.37 ± 0.03*	-	-	1.31 ± 0.02*	1.22 ± 0.03*	1.62 ± 0.02*	1.24 ± 0.03*
T_1	0.75 ± 0.02	0.70 ± 0.03	1.80 ± 0.02*	1.72 ± 0.04*	1.06 ± 0.02*	0.95 ± 0.01*	1.29 ± 0.02*	1.13 ± 0.03*	1.14 ± 0.02*	0.94 ± 0.04*
T_2	0.74 ± 0.03	0.70 ± 0.03	1.90 ± 0.02*	1.84 ± 0.03*	1.03 ± 0.02*	0.91 ± 0.02*	1.20 ± 0.01*	0.96 ± 0.03*	0.99 ± 0.01*	0.83 ± 0.04*
T_3	0.73 ± 0.03*	0.67 ± 0.02*	2.04 ± 0.02*	1.98 ± 0.03*	1.00 ± 0.02*	0.91 ± 0.02*	1.08 ± 0.02*	0.86 ± 0.03*	0.97 ± 0.02*	0.82 ± 0.04*
T_4	0.70 ± 0.02	0.66 ± 0.02	2.09 ± 0.02*	2.00 ± 0.03*	0.97 ± 0.01*	0.88 ± 0.01*	1.06 ± 0.02*	0.78 ± 0.02*	0.81 ± 0.02	0.80 ± 0.05
T_5	0.69 ± 0.03	0.65 ± 0.03	2.13 ± 0.01*	2.03 ± 0.03*	0.96 ± 0.01*	0.86 ± 0.03*	0.96 ± 0.02*	0.73 ± 0.02*	0.86 ± 0.02	0.86 ± 0.05
T_6	0.68 ± 0.02	0.65 ± 0.03	2.16 ± 0.02*	2.06 ± 0.03*	0.92 ± 0.02*	0.84 ± 0.01*	0.88 ± 0.02*	0.65 ± 0.02*	0.75 ± 0.02	0.70 ± 0.05
T_7	0.68 ± 0.02	0.64 ± 0.03	2.19 ± 0.02*	2.10 ± 0.02*	0.90 ± 0.02*	0.80 ± 0.02*	0.86 ± 0.01*	0.63 ± 0.02*	0.74 ± 0.02	0.69 ± 0.05
T_8	0.67 ± 0.02	0.63 ± 0.03	2.26 ± 0.02*	2.15 ± 0.04*	0.89 ± 0.02*	0.79 ± 0.02*	0.86 ± 0.02*	0.62 ± 0.02*	0.73 ± 0.02*	0.64 ± 0.06*
T_9	0.66 ± 0.02	0.63 ± 0.02	2.32 ± 0.02*	2.18 ± 0.03*	0.86 ± 0.02*	0.77 ± 0.01*	0.85 ± 0.02*	0.61 ± 0.02*	0.72 ± 0.02*	0.61 ± 0.03*
T_{10}	0.76 ± 0.02	0.73 ± 0.04	2.34 ± 0.01*	2.23 ± 0.03*	0.84 ± 0.01*	0.76 ± 0.01*	0.83 ± 0.02*	0.60 ± 0.02*	0.71 ± 0.02*	0.59 ± 0.03*
T_{11}	0.72 ± 0.02	0.70 ± 0.03	2.36 ± 0.02*	2.27 ± 0.03*	0.94 ± 0.02*	0.89 ± 0.03*	0.80 ± 0.01*	0.59 ± 0.01*	0.70 ± 0.01*	0.59 ± 0.04*
T_{12}	0.70 ± 0.02	0.70 ± 0.03	2.39 ± 0.01*	2.32 ± 0.02*	0.84 ± 0.02	0.83 ± 0.02	0.98 ± 0.02*	0.83 ± 0.04*	0.75 ± 0.03*	0.62 ± 0.04*
S_1	0.69 ± 0.03	0.69 ± 0.03	2.35 ± 0.02*	1.95 ± 0.05*	0.78 ± 0.02*	0.73 ± 0.02*	1.14 ± 0.02*	0.89 ± 0.02*	0.86 ± 0.02*	0.72 ± 0.03*
Cd-S_1	0.68 ± 0.03	0.67 ± 0.03	2.29 ± 0.03*	1.92 ± 0.04*	0.77 ± 0.02*	0.69 ± 0.01*	1.12 ± 0.02*	0.82 ± 0.02*	0.96 ± 0.01*	0.81 ± 0.03*
Cd-S_2	0.67 ± 0.03	0.67 ± 0.04	2.21 ± 0.02*	1.82 ± 0.04*	0.75 ± 0.03*	0.68 ± 0.01*	1.10 ± 0.02*	0.77 ± 0.03*	0.84 ± 0.02*	0.67 ± 0.04*
Cd-S_3	0.67 ± 0.03	0.65 ± 0.04	2.17 ± 0.02*	1.80 ± 0.03*	1.04 ± 0.02*	0.92 ± 0.02*	1.00 ± 0.02*	0.67 ± 0.02*	0.82 ± 0.03*	0.62 ± 0.02*
Cd_1	0.66 ± 0.02	0.64 ± 0.05	2.11 ± 0.02*	1.76 ± 0.03*	1.08 ± 0.02*	0.95 ± 0.01*	0.90 ± 0.02*	0.59 ± 0.04*	0.81 ± 0.02*	0.57 ± 0.04*
Cd_2	0.65 ± 0.02	0.64 ± 0.05	1.98 ± 0.01*	1.73 ± 0.04*	1.18 ± 0.02*	1.02 ± 0.01*	0.84 ± 0.02*	0.55 ± 0.02*	0.74 ± 0.02*	0.53 ± 0.04*
Cd_3	0.61 ± 0.02	0.64 ± 0.04	1.85 ± 0.02*	1.66 ± 0.03*	1.42 ± 0.02*	1.21 ± 0.03*	0.75 ± 0.03*	0.49 ± 0.02*	0.72 ± 0.03*	0.47 ± 0.03*
Cd_4	0.59 ± 0.01	0.62 ± 0.05	1.80 ± 0.02*	1.62 ± 0.02*	1.41 ± 0.02*	1.20 ± 0.02*	0.72 ± 0.02*	0.48 ± 0.02*	0.68 ± 0.02*	0.44 ± 0.04*
Cd_5	0.59 ± 0.01	0.61 ± 0.05	1.78 ± 0.01*	1.60 ± 0.03*	1.39 ± 0.02*	1.18 ± 0.01*	0.69 ± 0.01*	0.47 ± 0.02*	0.66 ± 0.02*	0.41 ± 0.04*
Cd_6	0.58 ± 0.01	0.61 ± 0.04	1.75 ± 0.02*	1.57 ± 0.04*	1.39 ± 0.02*	1.17 ± 0.01*	0.67 ± 0.01*	0.46 ± 0.02*	0.63 ± 0.01*	0.40 ± 0.04*
Cd_7	0.58 ± 0.02	0.59 ± 0.04	1.74 ± 0.02*	1.53 ± 0.03*	1.38 ± 0.02*	1.16 ± 0.01*	0.66 ± 0.02*	0.44 ± 0.02*	0.62 ± 0.02*	0.39 ± 0.04*
Cd_8	0.57 ± 0.01	0.57 ± 0.04	1.73 ± 0.02*	1.52 ± 0.02*	1.30 ± 0.02*	1.14 ± 0.01*	0.64 ± 0.02*	0.42 ± 0.02*	0.60 ± 0.02*	0.37 ± 0.05*
Cd_9	0.56 ± 0.02	0.56 ± 0.03	1.70 ± 0.02*	1.49 ± 0.03*	1.28 ± 0.02*	1.13 ± 0.02*	0.62 ± 0.02*	0.41 ± 0.02*	0.58 ± 0.02*	0.37 ± 0.04*
Cd_{10}	0.56 ± 0.02	0.55 ± 0.03	1.67 ± 0.02*	1.46 ± 0.03*	1.26 ± 0.02*	1.12 ± 0.01*	0.58 ± 0.02*	0.40 ± 0.02*	0.55 ± 0.01*	0.36 ± 0.04*
Cd_{11}	0.55 ± 0.02	0.51 ± 0.04	1.65 ± 0.02*	1.45 ± 0.02*	1.17 ± 0.01*	1.09 ± 0.01*	0.56 ± 0.02*	0.38 ± 0.02*	0.52 ± 0.02*	0.33 ± 0.04*
Cd_{12}	0.54 ± 0.02*	0.49 ± 0.03*	1.61 ± 0.01*	1.40 ± 0.04*	1.15 ± 0.02*	1.06 ± 0.03*	0.55 ± 0.02*	0.37 ± 0.02*	0.52 ± 0.01*	0.32 ± 0.04*
Cd_{13}	0.54 ± 0.02*	0.47 ± 0.03*	1.59 ± 0.02*	1.35 ± 0.02*	1.11 ± 0.01*	1.01 ± 0.02*	0.53 ± 0.01*	0.32 ± 0.03*	0.49 ± 0.02*	0.31 ± 0.04*
Cd_{14}	0.52 ± 0.02*	0.47 ± 0.03*	1.44 ± 0.02*	1.34 ± 0.02*	1.07 ± 0.01*	0.96 ± 0.01*	0.52 ± 0.01*	0.31 ± 0.02*	0.48 ± 0.01*	0.31 ± 0.05*
Cd_{15}	0.52 ± 0.02*	0.46 ± 0.03*	1.41 ± 0.02*	1.33 ± 0.02*	1.05 ± 0.02*	0.93 ± 0.02*	0.51 ± 0.02*	0.30 ± 0.02*	0.46 ± 0.01*	0.30 ± 0.04*
Cd_{16}	0.51 ± 0.02*	0.43 ± 0.03*	1.37 ± 0.03*	1.32 ± 0.01*	1.01 ± 0.02*	0.89 ± 0.01*	0.49 ± 0.02*	0.29 ± 0.02*	0.44 ± 0.02*	0.28 ± 0.04*
Cd_{17}	0.50 ± 0.02*	0.41 ± 0.03*	1.35 ± 0.02*	1.28 ± 0.02*	0.98 ± 0.02*	0.85 ± 0.02*	0.48 ± 0.02*	0.27 ± 0.01*	0.42 ± 0.02*	0.27 ± 0.03*
Cd_{18}	0.49 ± 0.02*	0.40 ± 0.03*	1.25 ± 0.01	1.23 ± 0.03	0.91 ± 0.02*	0.80 ± 0.02*	0.47 ± 0.02*	0.26 ± 0.01*	0.41 ± 0.01*	0.26 ± 0.03*
Cd_{19}	0.48 ± 0.02*	0.38 ± 0.03*	1.22 ± 0.01	1.21 ± 0.03	0.83 ± 0.02*	0.75 ± 0.01*	0.45 ± 0.02*	0.24 ± 0.01*	0.39 ± 0.02*	0.25 ± 0.03*
Cd_{20}	0.46 ± 0.02*	0.36 ± 0.04*	1.17 ± 0.01	1.15 ± 0.02	0.80 ± 0.02*	0.73 ± 0.02*	0.44 ± 0.02*	0.24 ± 0.01*	0.37 ± 0.02*	0.24 ± 0.02*
Cd_{21}	0.45 ± 0.02*	0.35 ± 0.03*	1.11 ± 0.02	1.08 ± 0.04	0.76 ± 0.01*	0.70 ± 0.02*	0.43 ± 0.02*	0.23 ± 0.01*	0.37 ± 0.02*	0.23 ± 0.03*
Cd_{22}	0.38 ± 0.02	0.34 ± 0.03	1.04 ± 0.02	1.05 ± 0.03	0.68 ± 0.02*	0.62 ± 0.03*	0.42 ± 0.02*	0.22 ± 0.01*	0.36 ± 0.03*	0.21 ± 0.03*
Cd_{23}	0.34 ± 0.02	0.32 ± 0.03	0.97 ± 0.02*	1.04 ± 0.03*	0.65 ± 0.02*	0.61 ± 0.02*	0.41 ± 0.02*	0.20 ± 0.01*	0.35 ± 0.02*	0.19 ± 0.02*
Cd_{24}	0.32 ± 0.02	0.31 ± 0.02	0.91 ± 0.03	0.97 ± 0.04	0.63 ± 0.02*	0.57 ± 0.02*	0.40 ± 0.02*	0.19 ± 0.01*	0.34 ± 0.02*	0.18 ± 0.01*
Cd_{25}	0.31 ± 0.02	0.31 ± 0.02	0.85 ± 0.02*	0.95 ± 0.03*	0.59 ± 0.02*	0.52 ± 0.03*	0.38 ± 0.02*	0.18 ± 0.00*	0.33 ± 0.02*	0.16 ± 0.03*
Cd_{26}	0.29 ± 0.02	0.29 ± 0.03	0.82 ± 0.02	0.85 ± 0.04	0.57 ± 0.01*	0.49 ± 0.02*	0.36 ± 0.02*	0.16 ± 0.01*	0.30 ± 0.02	0.15 ± 0.08
Cd_{27}	0.27 ± 0.02	0.28 ± 0.03	0.78 ± 0.01	0.79 ± 0.02	0.50 ± 0.03*	0.42 ± 0.01*	0.34 ± 0.02*	0.15 ± 0.01*	0.28 ± 0.02*	0.14 ± 0.02*
Cd_{28}	0.25 ± 0.02	0.27 ± 0.03	0.76 ± 0.02	0.76 ± 0.02	0.48 ± 0.02*	0.40 ± 0.01*	0.32 ± 0.03*	0.13 ± 0.01*	0.27 ± 0.02*	0.13 ± 0.02*
Cd_{29}	0.24 ± 0.01	0.26 ± 0.04	0.74 ± 0.01	0.74 ± 0.02	0.45 ± 0.03*	0.35 ± 0.01*	0.32 ± 0.02*	0.12 ± 0.01*	0.26 ± 0.02*	0.13 ± 0.01*
Cd_{30}	0.22 ± 0.01	0.25 ± 0.04	0.72 ± 0.01	0.70 ± 0.02	0.41 ± 0.04*	0.31 ± 0.01*	0.30 ± 0.03*	0.11 ± 0.01*	0.25 ± 0.02*	0.12 ± 0.02*
Cd_{31}	0.21 ± 0.01	0.21 ± 0.02	0.72 ± 0.01	0.64 ± 0.03	0.41 ± 0.02	0.26 ± 0.00	0.32 ± 0.02	0.10 ± 0.01	0.25 ± 0.01	0.10 ± 0.02

VBH: Vertebral body height; VBL: Vertebral body length; SPH: Spinous process height; SCW: Spinal canal width; and SCH: Spinal canal height.

* The asterisk in male and female samples for each parameter indicates a significant difference ($p < 0.05$) in the mentioned parameter between the two genders for the respective vertebra.

The atlas vertebra lacks a spinous process; therefore, SPH was absent in this vertebra of both sexes.

The highest SPH was recorded for Cd_3, while the lowest SPH was observed in the last caudal vertebra in both sexes.

No significant differences between males and females were found in T_{12} and Cd_{31} in all other vertebrae; SPH was greater in females than males (Table 2).

Spinal canal width (SCW) analysis. In female specimens, no significant differences in SCW were observed in the following comparisons: T_1 compared to the atlas and T_2 compared to the T_1. Significant differences were observed in T_3 compared to the T_2 and T_5 compared to the T_4, where SCW decreased in both cases, T_{12} compared to the T_{11} and S_1 compared to the T_{12}, where SCW increased in both cases, and Cd-S_3 compared to the Cd-S_2, Cd_1 compared to the Cd-S_3, and Cd_3 compared to the Cd_2, where SCW decreased in all cases. No significant differences were observed in T_4 compared to the T3, from T_6 to T_{11}, Cd-S_1 compared to the S_1, Cd-S_2 compared to the Cd-S_1, Cd_2 compared to the Cd_1, and from Cd_4 to the end of the vertebral column.

In male specimens, no significant differences in SCW were observed from atlas to T_4. Significant differences were found in the following comparisons: T_6 compared to the T_5, where SCW decreased, T_{12} compared to the T_{11}, where SCW increased, and Cd-S_1 compared to the S_1, Cd-S_3 compared to the Cd-S_2, and Cd_1 compared to the Cd-S_3, where SCW decreased in all cases. No significant differences were observed from T_7 to T_{10}, S_1 compared to the T_{12}, Cd-S_2 compared to the Cd-S_1, and from Cd_1 to the end of the vertebral column. The highest SCW was recorded in the atlas and the lowest SCW was observed in the last caudal vertebra in both males and females. No significant differences between males and females were found in Cd_{31} in all other vertebrae; SCW was greater in females than males (Table 2).

Spinal canal height (SCH) analysis. In female specimens, significant differences in SCH were observed in the following comparisons: T_1 compared to the atlas, T_2 compared to the T1, T_4 compared to the T_3, and T_6 compared to the T_5, where SCH decreased in all cases, and S_1 compared to the T_{12} and Cd-S_1 compared to the S_1, where SCH increased in both cases. In contrast, Cd-S_2 compared to the Cd-S_1 showed a decrease in SCH**.**

In comparisons between T_3 and T_2, T_5 and T_4, and all vertebrae from T_7 to T_{12}, no statistically significant differences in SCH were observed. Similarly, from Cd-S_3 to the last caudal vertebra, SCH did not differ significantly between adjacent vertebrae.

In male specimens, no statistically significant differences in SCH were found between any adjacent vertebrae throughout the entire vertebral column.

The maximum SCH in both male and female specimens was recorded in the atlas, while the minimum SCH was observed in the last caudal vertebra.

When comparing SCH between sexes, no significant differences were observed in T_4, T_5, T_6, T_7, Cd_{26}, and Cd_{31}, while the differences were statistically significant in all other vertebrae. In those vertebrae, SCH was consistently greater in females than males (Table 2).

Discussion

In a microscopic study conducted by Khoshnamvand *et al*. on the Luristan newt, it was reported that the species has two cervical vertebrae, 16 abdominal vertebrae, and 32 caudal vertebrae.[12] However, the findings from the present study, based on the micro-CT scanning, revealed the presence of one cervical vertebra, 12 trunk vertebrae, one sacral vertebra, three caudo-sacral vertebrae, and a total of 28 - 31 vertebrae. Utilizing advanced micro-CT technology for both 2D and 3D imaging, this study was able to identify detailed micro-anatomical structures that were previously underexplored in earlier research.

Several morphological features similar to those examined in this study have been reported in other research, including "Osteology of the Italian Endemic Spectacled Salamanders", "Osteology of Mountain Stream Salamanders from Western China", and "Osteological Characteristics of the Setouchi Salamander".[13-15] Additionally, several morphological parameters studied here had not been investigated in amphibian or reptile samples until the presentation of this study. Therefore, the morphological parameters in this study are compared with a mammalian species, the New Zealand rabbit.

The number of cervical vertebrae in Luristan newt is consistent with studies conducted on mountain stream salamanders from Western China, Italian native salamanders, and the Setouchi salamander, in all of which a single cervical vertebra was observed. In contrast, the New Zealand rabbit has seven cervical vertebrae.[13-16]

In the osteological study of the mountain stream salamanders from Western China, it was found that they have 16 trunk vertebrae, while the Setouchi salamander has 15 - 16 trunk vertebrae and Italian native salamanders have 12 - 13 trunk vertebrae. However, all specimens of Luristan newt, like the New Zealand rabbit, exhibited 12 trunk (thoracic) vertebrae, with each of these vertebrae possessing a pair of ribs attached to the anterior region.[13-15,17]

In Luristan newt, and in studies conducted on the mountain stream salamanders from Western China, Setouchi salamander, and Italian native salamanders, no lumbar vertebrae were present. In contrast, the New Zealand rabbit has seven lumbar vertebrae.[13-15,18]

Unlike the New Zealand rabbit, which has four sacral vertebrae, the Luristan newt, mountain stream salamanders from Western China, Setouchi salamander, and Italian native salamanders have only one sacral vertebra.[13-15,18]

In both male and female Luristan newts, the difference in VBH between the T_9 and T_{10} vertebrae was significant, while this difference was not significant across the thoracic vertebrae of the New Zealand rabbit.[17] The VBH in the trunk vertebrae of Luristan newt was the highest in T_{12} for both males and females. The smallest VBH in the Luristan newt's trunk vertebrae was found in T_9 for both sexes. In the Luristan newt, the VBH in the Cd_{18}, T_3, Cd_{12}, Cd_{13}, Cd_{14}, Cd_{15}, Cd_{16}, Cd_{17}, Cd_{18}, Cd_{19}, Cd_{20}, and Cd_{21} vertebrae was greater in females than males, while in the other vertebrae, the sizes were equal.

The difference in VBL across the thoracic vertebrae of the New Zealand rabbit was significant only in T_{12} compared to the other thoracic vertebrae, where the size increased at T_{12}.[17] In contrast, in the trunk vertebrae of the Luristan newt (both male and female), the VBL differences were significant between several vertebrae. The largest VBL in the Luristan newt's trunk vertebrae, similar to the thoracic vertebrae of the New Zealand rabbit, was observed in T_{12}.[17] The smallest VBL in the thoracic vertebrae of the New Zealand rabbit was found in T_7, whereas the smallest VBL in the trunk vertebrae of the Luristan newt was observed in T_1 (both sexes).[17] The VBL in the Cd_{18}, Cd_{19}, Cd_{20}, Cd_{21}, Cd_{22}, Cd_{24}, Cd_{26}, Cd_{27}, Cd_{28}, Cd_{29}, Cd_{30}, and Cd_{31} vertebrae was equal between both sexes of the Luristan newt. In the Cd_{23} and Cd_{25} vertebrae, the VBL in males was larger than females, while in other vertebrae, the VBL in females was larger than males.

In the Setouchi salamander, the length of the vertebrae from the atlas to T_4 increased, while in the Italian native salamanders, the anterior trunk vertebrae were shorter than the posterior ones.[13,15] In the mountain stream salamanders from Western China, the trunk vertebrae showed unequal lengths.[14] However, in the Luristan newt (both male and female), the length of the vertebrae increased from the atlas to T_3. In female Luristan newt, similar to the Setouchi salamander, Italian native salamanders, and mountain stream salamanders from Western China, the sacral vertebra was of similar length to the trunk vertebrae; while, in male Luristan newt, the sacral vertebra was shorter than the trunk vertebrae.[13-15]

In the New Zealand rabbit, the difference in SPH between the 2nd and 3rd thoracic vertebrae and other vertebrae was significant, whereas in the Luristan newt (both male and female), this difference was significant between T_{10} and T_{12}.[17] The highest SPH in the thoracic vertebrae of the New Zealand rabbit was observed in T_3; while, in the Luristan newt, the highest SPH in the trunk vertebrae was observed in T_1.[17] The lowest SPH in the trunk vertebrae of the Luristan newt (both males and females) was observed in T_{10}. The highest SPH in the vertebral column of the Luristan newt was found in Cd_3. The SPH in T_{12} and Cd_{31} vertebrae was the same in both sexes, and in the other vertebrae, the SPH was larger in females than males.

In the New Zealand rabbit, the difference in SCW between the thoracic vertebrae was not significant, whereas in the trunk vertebrae of the Luristan newt (both male and female), the difference in SCW between several vertebrae was significant.[17] The highest SCW in the trunk vertebrae of the Luristan newt (both male and female) was found in T_1. The highest SCW in the entire column was observed in the atlas vertebra, while the lowest was found in the last caudal vertebra. The SCW in Cd_{31} was the same in both sexes, and in other vertebrae, the SCW was larger in females than males.

The size difference of SCH in the trunk vertebrae of male Luristan newt was not significant compared to the thoracic vertebrae of New Zealand rabbit, while the size difference of SCH in the trunk vertebrae of female Luristan newt was significant between several vertebrae.[17] The largest size of SCH in the vertebral column in both males and females was observed in the atlas vertebra, while the smallest size was observed in the last caudal vertebra. The size of SCH in T_4, T_5, T_6, T_7, Cd_{26}, and Cd_{31} was equal between genders, whereas in other vertebrae, the size of SCH in females was larger than males.

Anatomical studies and imaging of the internal structures of animals, such as the skeletal structure, form the basis of many biological and biomedical studies. Traditional methods, such as dissection, although are generally accessible and economically cost-effective, are considered invasive techniques that are unsuitable for studying endangered species and other valuable wildlife. In contrast, radiographic imaging and CT are less invasive and more efficient methods for studying internal structures in their precise anatomical positions. In this study, micro-CT scanning was employed for the first time in Luristan newt morphometry as a very accurate and less invasive method compared to the traditional methods, like dissection, thereby providing comprehensive and detailed information about the vertebral column characteristics of this salamander species in both males and females.

The study demonstrated that the average body length, tail length, and trunk length in males were smaller than those in females, indicating that females had larger body sizes compared to the males. Although females possess longer tails than males, this study found that males have a higher number of caudal vertebrae than females. In summary, this study found that males have smaller body sizes compared to the females. It is also noteworthy that no specimens were sacrificed during the study, and all samples were handed over to the relevant organization following completion of the experiment.

Acknowledgments

The authors wish to express their appreciation to everyone who assisted in this study, especially the staff of the Anatomy Division of the Faculty of Veterinary

Medicine, University of Tehran, Tehran, Iran, and Radiology Department of the Faculty of Veterinary Medicine, Science and Research Branch, Islamic Azad University, Tehran, Iran.

Conflict of interest

The authors declare that there is no conflict of interest regarding the publication of this article.

References

1. Simpson GG. Tempo and mode in evolution. 1st ed. New York, USA: Columbia University Press 1984; 100-234.
2. Facey DE, Bowen BW, Collette BB, et al. The diversity of fishes: biology, evolution and ecology. 2nd ed. Hoboken, USA: John Wiley & Sons 2022; 32-52.
3. Kardong KV. Vertebrates: comparative anatomy, function, evolution. 4th ed. New York, USA: McGraw-Hill 2006; 294-324.
4. Rastegar-Pouyani N, Kami HG, Rajabzadeh HR, et al. Annotated checklist of amphibians and reptiles of Iran. Iran J Anim Biosyst 2008; 4(1): 7-30.
5. Mobaraki A, Amiri M, Alvandi R, et al. A conservation reassessment of the critically endangered, Lorestan newt *Neurergus kaiseri* (Schmidt 1952) in Iran. ARC 2014; 9(1): 16-25.
6. Valizadeh Y, Nasrolahzadeh Masouleh M, Zehtabvar O, et al. Micro-CT anatomy of the vertebral column of the Luristan newt (Neurergus kaiseri). Vet Med Int 2025; 2025: 6958388. doi: 10.1155/vmi/6958388.
7. Ritman EL. Current status of developments and applications of micro-CT. Ann Rev Biomed Eng 2011; 13: 531-552.
8. Khoshnamvand H, Malekian M, Keivany Y. Morphological distinction and sexual dimorphism in divergent clades of *Neurergus kaiseri* (Amphibia: Salamandridae). Basic Appl Herpetol 2018; 32: 5-17.
9. Meredith A, Redrobe S. BSAVA manual of exotic pets. 4th ed. Gloucester, UK: British Small Animal Veterinary Association 2002; 331-337.
10. Bahin Negara Company. Available at: https://behin negareh.com. Accessed Nov 6, 2025.
11. Worthington RD, Wake DB. Patterns of regional variation in the vertebral column of terrestrial salamanders. J Morphol 1972; 137(3): 257-277.
12. Khoshnamvand H, Malekian M, Keivany Y, et al. Descriptive osteology of an imperiled amphibian, the Luristan newt (*Neurergus kaiseri*, Amphibia: Salamandridae). Acta Herpetol 2019; 14(1): 51-56.
13. Macaluso L, Villa A, Pitruzzella G, et al. Osteology of the Italian endemic spectacled salamanders, Salamandrina spp. (Amphibia, Urodela, Salamandridae): selected skeletal elements for palaeontological investigations. J Morphol 2020; 218(11): 1391-1410.
14. Jia J, Jiang JP, Zhang MH, et al. Osteology of *Batrachuperus yenyuanensis* (Urodela, Hynobiidae), a high-altitude mountain stream salamander from western China. PLoS One 2019; 14(1): e0211069. doi: 10.1371/journal.pone.0211069.
15. Hara S, Nishikawa K. Osteological characteristics of the Setouchi salamander *Hynobius setouchi* (Urodela, Hynobiidae). Anat Rec (Hoboken) 2022; 305(6): 1316-1342.
16. Shateri-Amiri B, Soroori S, Zehtabvar O, et al. Computed tomographic and morphometric study of cervical vertebrae in healthy white New Zealand rabbit (*Oryctolagus Cuniculus*). Iran J Vet Med 2020; 14(4): 421-432.
17. Soroori S, Zehtabvar O, Amiri BS, et al. Evaluation of thoracic vertebrae in healthy White New Zealand rabbit (*Oryctolagus Cuniculus*): computed tomographic and morphometric study. Vet Med Sci 2022; 5(5): 1950-1957.
18. Soroori S, Zehtabvar O, Shateri-Amiri B, et al. Computed tomographic and morphometric study of lumbosacral and coccygeal vertebrae in healthy White New Zealand rabbit (*Oryctolagus Cuniculus*). Iran J Vet Surg 2022; 17(1): 55-61.